New Insights Into Steam/Solvent-Coinjection-Process Mechanism

Raman K. Jha, SPE; **Mridul Kumar,** SPE; **Ian Benson,** SPE; and **Edward Hanzlik,** SPE;
Chevron Energy Technology Company

Summary

We present results of a detailed investigation of the steam/solvent-coinjection-process mechanism by use of a numerical model with homogeneous reservoir properties and various solvents. We describe condensation of steam/solvent mixture near the chamber boundary. We present a composite picture of the important phenomena occurring in the different regions of the reservoir and their implications for oil recovery. We compare performances of various solvents and explain the reasons for the observed differences. An improved understanding of the process mechanism will help with selecting the best solvent and developing the best operating strategy for a given reservoir.

Results indicate that as the temperature drops near the chamber boundary, steam starts condensing first because its mole fraction in the injected steam/solvent mixture (and hence its partial pressure and the corresponding saturation temperature) is much higher than the solvent's. As temperature declines toward the chamber boundary and steam continues to condense, the vapor phase becomes increasingly richer in solvent. At the chamber boundary where the temperature becomes equal to the condensation temperature of both steam and solvent at their respective partial pressures, both condense simultaneously. Thus, contrary to steam-only injection, where condensation occurs at the injected steam temperature, condensation of steam/solvent mixture is accompanied by a reduction in temperature in the condensation zone and the farther regions. However, there is little change in temperature in the central region of the steam chamber.

The condensed steam/solvent mixture drains outside the chamber, leading to the formation of a mobile liquid stream (drainage region) where heated oil, condensed solvent, and water flow together to the production well. The condensed solvent mixes with the heated oil and further reduces its viscosity. The additional reduction in viscosity by solvent more than offsets the effect of reduced temperature near the chamber boundary. As the steam chamber expands laterally because of continued injection and as temperature in the hitherto drainage region increases, a part of the condensed solvent mixed with oil evaporates. This lowers the residual oil saturation (ROS) in the steam chamber. Therefore, ultimate oil recovery with the steam/solvent-coinjection process is higher than that in steam-only injection. The higher the solvent concentration in oil at a location, the greater is the reduction in the ROS there. Our explanation is corroborated by the experimental results reported in the literature, which show smaller ROS in the steam chamber after a steam/solvent-coinjection process.

A lighter solvent has a lower viscosity, a higher volatility, and a higher molar concentration of solvent in the drainage region. Thus, a lighter solvent causes a greater reduction in the viscosity of the heated oil and also leads to a lower ROS. Therefore, the lightest condensable solvent (butane, under the conditions investigated) provides the most favorable results in terms of enhancements in oil rate and oil recovery. This is different from the prior claims in the literature.

This paper (SPE 159277) was accepted for presentation at the SPE Annual Technical Conference and Exhibition, San Antonio, Texas, USA, 8–10 October 2012, and revised for publication. Original manuscript received for review 18 June 2012. Revised manuscript received for review 8 March 2013. Paper peer approved 26 March 2013.

Introduction

Steam-assisted gravity drainage (SAGD) has become the preferred technology for exploiting the huge resource base of bitumen. There are more than 10 commercial SAGD projects in Canada. The field performance indicates that the process offers high production rate and high ultimate recovery. However, it requires a large volume of steam injection. The observed steam/oil ratio (SOR) in the field is in the range of 3 to 5 cold water equivalent (CWE) bbl/STB (Jimenez 2008). A large usage of steam can affect the project economics adversely and also can have a detrimental impact on the environment.

There have been numerous studies that aim to improve SAGD's performance. These involve variations in the well configuration or changes in the operating methodology. In particular, steam/solvent coinjection appears promising. In this process, a small amount of vaporized but condensable hydrocarbon solvent is added to steam (Nasr et al. 2003). Laboratory investigation (Nasr and Ayodele 2005, 2006) and field trials (**Table 1**) have demonstrated that compared with steam-only injection, adding solvent to steam results in higher oil rate, reduced SOR, and higher ultimate recovery.

Table 1 presents a brief summary of the previous field trials of steam/solvent coinjection. Although none of the pilots [except the LASER (liquid addition to steam for enhanced recovery) pilot by Imperial Oil] has been conducted long enough to provide conclusive results, they generally indicate much-improved performance. This technique may prove invaluable in overcoming some of SAGD's shortcomings.

Steam/solvent coinjection is a complex process. A successful and profitable field implementation requires a judicious decision about solvent type, solvent concentration, and the operating strategy. Selection of the optimum set of parameters is difficult because of a large number of variables involved and their nonlinear effect on the economic performance (Edmunds et al. 2009). A thorough understanding of the oil-recovery mechanism is required for an improved design of the process and to gain maximum benefits of the technology.

This topic has attracted much research interest in the industry as well as in academia. Ardali et al. (2012) present a detailed review of prior studies. Although the effect of solvent addition on viscosity reduction is well described in the literature (Gates 2007; Deng et al. 2010), no other mechanistic details have been reported. There is a misunderstanding that a solvent with vaporization temperature comparable to that of steam will condense together with steam at the chamber boundary (Nasr et al. 2003). The misunderstanding of steam/solvent condensation leads to an incorrect selection of the most appropriate solvent. Furthermore, there is little information available about the formation of a mobile liquid stream (or drainage region) outside the steam-chamber boundary and the phenomena occurring in that region. Most importantly, the mechanism of increase in ultimate oil recovery by solvent addition to steam is not well understood (Nasr and Ayodele 2006). It often leads to an inappropriate representation of ROS in numerical-simulation studies and may result in erroneous conclusions.

This study fills some of the gaps to develop an improved understanding of the steam/solvent-coinjection process. We have carried out a detailed investigation of the process mechanism by use of a fine-grid numerical model with homogeneous reservoir properties and various solvents. We describe condensation of the

TABLE 1—SUMMARY OF PREVIOUS FIELD TRIALS OF SOLVENT COINJECTION WITH STEAM

Project	Operator	Steam-Injection Mode	Solvent	Oil Rate		SOR		Comments	References
				Before Solvent	After Solvent	Before Solvent	After Solvent		
Senlac (2002)	EnCana	Continuous	Butane (15% by weight)	1,900 B/D	3,000 B/D	2.6	1.6	1. Pilot stopped prematurely after 2 months because of pressure depletion. 2. More than 70% solvent recovery. 3. 1°API improvement in gravity.	Gupta et al. (2005)
Christina Lake (2004)	EnCana	Continuous	Butane (15% by weight)	630 B/D	1,900 B/D	5	Less than 1	1°API improvement in gravity.	Gupta and Gittins (2006)
LASER (Cold Lake) (2002 to 2007)	Imperial Oil	Cyclic	Diluent (approximately 6% by volume)	1,570 B/D	2,830 B/D	3.45	2.56	1. A large-scale application started at Cold Lake in 240 wells. 2. Results of the first cycle consistent with prepilot expectations and simulation predictions.	Leaute and Carey (2007); Boone et al. (2011)
Tia Juana (1987)	PDVSA	Cyclic	Industrial diesel (5% by volume)	191 B/D	301 B/D	0.40	0.25	86% increase in cumulative production over a 30-month period.	Bracho and Oquendo (1991)
Firebag (2005)	Suncore	Continuous	Naphtha	—	—	—	—	1. No observed bitumen-production-rate increase. 2. The solvent, naphtha, was believed to be too heavy (mean carbon number of 8).	Orr (2009)

steam/solvent mixture near the chamber boundary. We present a composite picture of the important phenomena occurring in the different regions of the reservoir and explain the mechanism of improvement in oil rate and increase in recovery. We compare performances of various solvents and explain the reasons for the observed difference in their benefits. We corroborate our mechanistic model with experimental results and field data from the available literature. The model and an improved understanding of the process mechanism will help with selecting the best solvent and the best operating strategy for a given reservoir.

Model Description

Reservoir Model. The homogeneous model used in this study **(Fig. 1)** has the averaged reservoir properties for a field in Athabasca, Canada, as shown in **Table 2.** A homogeneous model enables us to separate the effects of reservoir geology and keeps focus explicitly on the phenomena occurring in the reservoir.

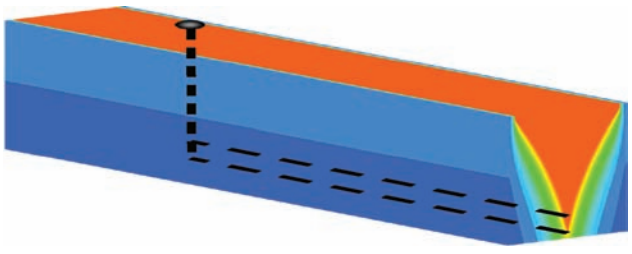

Fig. 1—Schematic of the reservoir model used in the current study.

Fluid Model. For ease of analysis and explanation of results, we use a simple fluid model to represent the reservoir fluid and injected solvents. The model captures the essential features of fluid phase behavior to describe the key phenomena occurring during the process. Some minor effects, such as asphaltene precipitation and mutual solubility of hydrocarbon and water, have not been considered.

The oil (bitumen) is a very high molecular weight, dead (involatile) component. Use of a dead-oil system makes the model similar to Butler's conceptual model of SAGD (Butler 1994). We acknowledge the importance of solution gas as indicated by a few researchers (Yuan et al. 2006; Sharma et al. 2012). However, solution gas makes it difficult to separate the effects of exsolved solution gas and the injected solvent. This simplification is useful in investigating key recovery mechanisms, and it also allows explanation of simulation results using simple phase behavior calculations. The simple mechanistic model described in this paper provides a strong foundation for including the impact of solution gas in the future.

TABLE 2—RESERVOIR-MODEL PROPERTIES

Porosity	0.30
Horizontal permeability	2,000 md
Vertical permeability	1,000 md
Water saturation	0.30
Irreducible water saturation (S_{wir})	0.30
Residual oil saturation to gas (S_{org})	0.15

TABLE 3—PSEUDOCOMPONENT AND PURE-COMPONENT PROPERTIES

	Propane	Butane	Pentane	Hexane	Heptane	Diluent	Octane	Decane	Syncrude	Bitumen
Molecular weight	44	58	72	86	100	104.5	114	142	203.4	600.00
Specific gravity	0.51	0.58	0.63	0.66	0.69	0.71	0.71	0.73	0.8670	1.01
Boiling point (°F)	–43.7	31.1	97.0	155.7	208.4	187.1	257.0	345.5	533.4	1015.0
Viscosity at injection temperature (cp)	0.0023	0.0310	0.0387	0.0625	0.0837	0.1000	0.1066	0.1568	0.3170	8.40
Antoine coefficient *A*	12.659	12.794	12.997	13.213	13.210	15.719	13.911	13.563	16.126	0
Antoine coefficient *B*	416.66	656.31	910.67	1164.16	1283.51	2829.1	1839.65	1842.53	4203.94	0
Antoine coefficient *C*	–192.714	–191.377	–173.267	–160.374	–166.867	–47.83	–129.799	–161.656	–109.7	0

We have examined several pure hydrocarbon solvents ranging from propane (C_3) to decane (C_{10}). We also investigate two industrial solvents: diluent and syncrude. Use of different solvents enables us to investigate the roles of solvent properties and their impact on the oil recovery in a generalized manner. All solvents (including the industrial solvents) are modeled as single pseudocomponents. Leaute and Carey (2007) have shown that use of a single pseudocomponent to represent a multicomponent diluent is a reasonable approximation.

The thermodynamic properties of pure components have been measured extensively and are available in several textbooks (Reid et al. 1986; NIST 2011). The pseudocomponent properties (for bitumen, diluents, and syncrude) are derived by use of standard correlations and the measured data. Important thermodynamic properties of all the components used in this study are shown in **Table 3.**

Phase-Behavior Calculations. The phase behavior of all components is described by use of Antoine's model (Reid et al. 1986). It is the most common approach to model fluid phase behavior of heavy oils. As per the Antoine equation, the vapor pressure of component i is related to temperature as

$$P_i = \exp\left[A_i - \frac{B_i}{T + C_i}\right], \quad \ldots\ldots\ldots\ldots\ldots\ldots\ldots\ldots (1)$$

where vapor pressure (P_i) is in mm Hg and temperature T is in K. A_i, B_i, and C_i are Antoine coefficients of the component i and are determined by fitting results of equation-of-state flash calculations (on dead oil, steam, and solvent mixture) with the Antoine model. Thus, the impact of fluid composition on K-values is implicitly modeled.

The Antoine coefficients of all the components are shown in Table 3. The calculated vapor-pressure curves of all the solvents are shown in **Fig. 2.** K-values for individual components are obtained by dividing the component vapor pressure by total system pressure ($K_i = P_i/P_t$). Despite its simplicity, the Antoine-equation approach models the K-values satisfactorily for oils of relatively low volatility (Hong and Hsueh 1987).

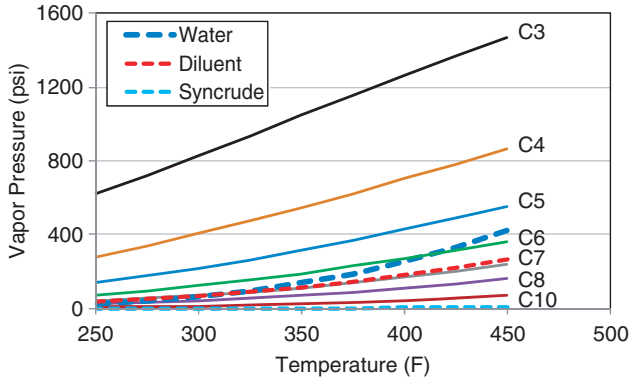

Fig. 2—Estimated vapor pressures of solvents used in current study.

At reservoir temperature of 46°F, oil viscosity is 1.6 million cp and it reduces to 8 cp at steam-injection temperature of 440°F. Solvent viscosities at steam-injection temperature are also shown in Table 3. Oil and condensed solvent are assumed to be first-contact miscible. The oil-phase viscosity is calculated from constituent-component viscosities by use of the ideal mixing rule,

$$\ln\mu_o = \sum x_i \ln\mu_{oi}, \quad \ldots\ldots\ldots\ldots\ldots\ldots\ldots\ldots (2)$$

where x_i is the mole fraction of component i in the oil phase and μ_{oi} is its viscosity.

Simulator. Chevron's in-house simulator, Chevron Extended Applications Reservoir Simulator (CHEARS), was used for this study. CHEARS is a 3D, fully implicit thermal compositional simulator. It accurately captures the fluid flow, heat transfer, and the fluid phase behavior (Chien et al. 1985). Simulation studies on steam/solvent coinjection reported in the literature have been successful in reproducing laboratory experiments and the field observations (Deng et al. 2010; Ivory et al. 2010). This supports the reliability of a simulator as a predictive and investigative tool for designing and analyzing the steam solvent co-injection process.

A simulator also enables visualization of the important phenomena occurring in the reservoir. It allows investigation of the roles of a number of process variables in a reasonable time and complements the experimental work reported in the literature.

Reservoir Grid. The model used in this study represents a 100-ft-thick reservoir with 490-ft (150-m) well spacing and a 2,600-ft-long horizontal well. The base-case grid sizes are $\Delta x = \Delta z = 3.28$ ft and $\Delta y = 1{,}300$ ft. The well is in the y-direction.

Because all the important process phenomena (e.g., heating, mixing, drainage) occur in the x–z plane, it is important to ensure that the results are not affected by the selection of the grid size. We conducted a sensitivity study on the grid size and determined that a grid size of 3.28×3.28 ft is adequate. This is consistent with the findings of Boak and Palmgren (2004). Use of smaller grid size (1.64×1.64 ft and 0.82×0.82 ft) does not alter the results significantly. However results obtained from a fine grid model (0.82 ft $\times 0.82$ ft in the x–z plane) are presented in this paper to obtain a better resolution of the phenomenoa occurring in the mixing zone. Results at this resolution have not been reported previously.

Injection and Production Conditions. Steam (90% quality at the sandface) and solvent are injected at a constant pressure of 400 psi throughout the investigation period. This was performed to ensure no change in pressure and temperature conditions in the steam chamber with time and hence no change in the solvent phase behavior.

The solvent/steam ratio was maintained at 5% w/w. **Table 4** shows the corresponding mole fractions of solvents in the injected mixture. It also shows the volume injection rate of the gaseous solvent for a steam-injection rate of 5,000 CWE B/D. The production well was constrained to keep the live-steam production limited to a small value.

TABLE 4—SOLVENT MOLE PERCENTAGE AND INJECTION RATES FOR VARIOUS SOLVENTS									
	Propane	Butane	Pentane	Hexane	Heptane	Diluent	Octane	Decane	Syncrude
Mole percentage	2.05	1.55	1.25	1.05	0.90	0.86	0.79	0.63	0.44
Injection rate (Mscf/D)	714	541	436	365	314	303	276	221	156

Steam-injection rate = 5000 CWE B/D; solvent concentration = 5% w/w.

Description of the Process Mechanism for SAGD

The SAGD process mechanism has been well investigated in the literature (Ito and Suzuki 1999; Aherne and Maini 2008). Yet a description of the SAGD mechanism from this study is presented first to establish a reference for comparison with steam/solvent-coinjection process and to illustrate our investigation methodology.

Fig. 3a shows a cross section of the fully developed steam chamber at a fixed time. A fully developed steam chamber in a dead-oil reservoir has a V-shape. Fig. 3a also shows an arbitrary observation line. As we move from the left end of the line to the right, we move from the midpoint of the steam chamber to the unperturbed, virgin portion of the reservoir. Figs. 3b through 3d plot several parameters of interest along this observation line. The three distinct regions of the reservoir—the steam chamber, the liquid-stream or drainage region adjacent to the steam-chamber boundary (discussed below), and the unperturbed region—are demarcated in different colors in Figs. 3b through 3d.

Variation of Pressure and Temperature Along the Observation Line (Fig. 3b). The left portion of the observation line that lies in the steam chamber has a constant temperature and pressure consistent with the injected-steam conditions.

The region beyond the steam chamber is conductively heated. The temperature declines as we move away from the steam-chamber boundary. At far enough distances in the unperturbed region of the reservoir, the temperature essentially declines to the original reservoir temperature. As seen in Fig. 3b, the thickness of the conductively heated zone is approximately 25 ft. This is consistent with the observation-well data (Birrell 2001) and calculations made by Sharma and Gates (2011).

Variations in Saturations Along the Observation Line (Fig. 3c). There is essentially no variation in the phase saturations in the steam chamber. The oil saturation is near the ROS. The water saturation in the steam chamber is slightly higher than the initial water saturation. The remaining pore space is occupied by steam (vapor phase).

At the boundary of the steam chamber, steam loses its latent heat to the reservoir and condenses. A sharp increase in the water saturation is observed at the chamber boundary. Moving along the observation line, the water saturation—in a short distance—declines from its maximum value at the chamber boundary to its in-situ value.

The reservoir in the unperturbed region is at the original reservoir conditions because the fluids in this region are essentially immobile.

Process Mechanism. Fig. 3d plots oil viscosity and mobility ($k \cdot k_r^o/\mu_o$) along the observation line. The oil viscosity increases

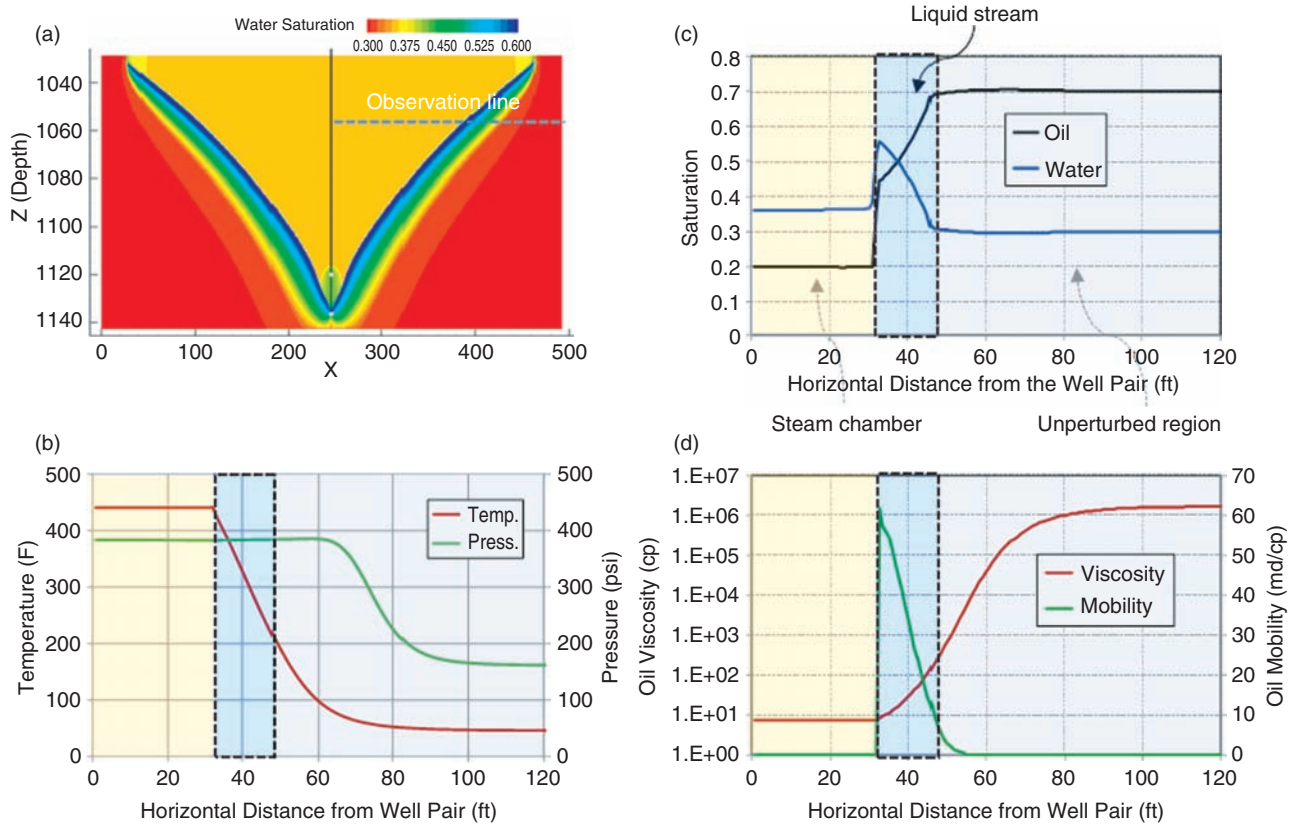

Fig. 3—Details of oil recovery with SAGD. (a) A cross section of steam chamber. Three distinct regions are identified in the reservoir—steam chamber, liquid stream, and unperturbed region—and are demarcated in different colors. (b) Variation in temperature and pressure along the observation line. (c) Variation of liquid saturations along the observation line. (d) Variation in oil viscosity and mobility. Oil mobility is limited to the liquid-stream region. In this region, the heated oil flows with water along the chamber boundary.

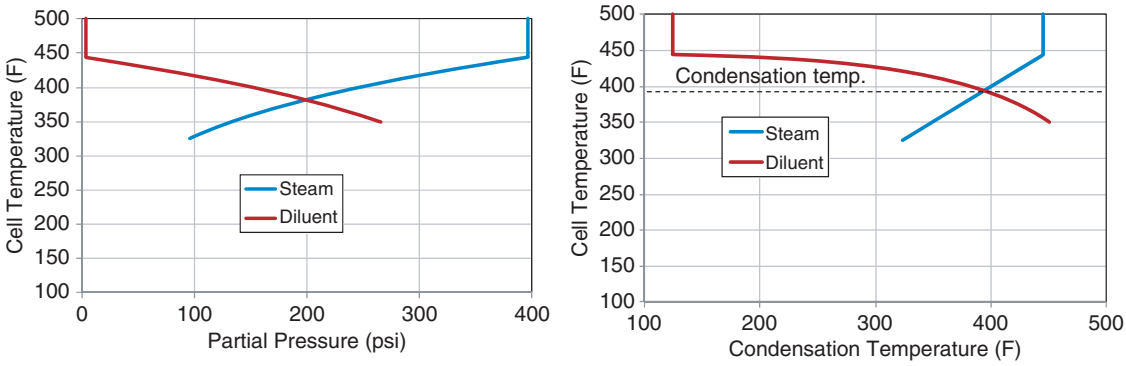

Fig. 4—Condensation of steam/diluent mixture (5% w/w solvent) in a PVT cell at 400 psi. Steam starts condensing when the cell temperature is reduced to 443.75°F. With further reduction in temperature, the vapor- and liquid-phase compositions change continuously. The condensation temperature of solvent rises as its mole fraction and its partial pressure increase. With a greater reduction in temperature, the vapor phase becomes increasingly richer in solvent. When the cell temperature reduces to 393°F, both components have partial pressures corresponding to their saturation temperature and condense together. At temperatures lower than this, steam and solvent (diluent) exist in liquid phase only.

dramatically as we move away from the steam chamber because of decreasing temperature. It is evident that oil is practically mobile only in a thin region of the reservoir adjacent to the steam-chamber boundary. This region is highlighted as "liquid stream" in Fig. 3c and it contains heated, mobile oil as well as the condensed steam. Farther away from this region, even though the reservoir is heated to some extent, the oil mobility is low because of its high viscosity.

Thus, condensation of steam at the chamber boundary and subsequent heating of oil in the neighboring region leads to the formation of a liquid stream. In the liquid-stream region, all the important dynamic-process phenomena occur. This is practically the only region where mobile fluids are present. Little liquid production occurs from the steam chamber or the unperturbed region. The fluids from the liquid stream flow down along the chamber boundary to the production well.

As the steam injection continues and the steam chamber expands, the whole arrangement shifts laterally outward.

Description of the Process Mechanism for SAGD With Solvent (Diluent)

Condensation of Steam and Solvent. One of the often misunderstood aspects of the steam/solvent-coinjection-process mechanism is the condensation of the injected mixture near the chamber boundary. It is believed that a solvent with vaporization temperature comparable to that of steam will condense together with steam at the chamber boundary (Nasr et al. 2003). This misunderstanding may lead to an erroneous conclusion about the selection of the most suitable solvent. Therefore, we first illustrate condensation of the steam/solvent mixture in a pressure/volume/temperature (PVT) cell by use of an approach similar to that of Dong (2012). The mixture is placed in the cell at its injection concentration. The pressure in the cell is maintained at the injection pressure throughout the study. The temperature of the cell is reduced slowly until the mixture condenses completely. This procedure mimics the condensation of the steam/solvent mixture near the chamber boundary.

Steam and solvent, being immiscible, do not interact with each other and may be assumed to behave ideally. As the temperature of the cell is reduced, each component condenses when the cell temperature equals the saturation (or condensation) temperature of the component at its own partial pressure.

For illustration, we use diluent as the solvent. A 5% w/w (0.86 mol% of diluent) mixture is cooled in the PVT cell at 400 psi. Because of a small mole fraction of solvent in the mixture ($y_{solv} = 0.0086$), the partial pressure of solvent ($P_{solv} = y_{solv} \times P_t = 0.0086 \times 400$ psi $= 3.44$ psi) is much smaller than that of steam ($P_{stm} = (1 - y_{solv}) \times P_t = 396.56$ psi). The saturation (or condensation) temperatures of steam and solvent corresponding to their prevailing partial pressures are 443.75 and 109.58°F, respectively. Therefore, steam starts condensing when the cell temperature is reduced to 443.75°F.

As the temperature of the cell is reduced further, the vapor- and liquid-phase compositions change continuously. As steam condenses, its mole fraction in the vapor phase (y_{stm}) and its partial pressure (P_{stm}) drop. This leads to a reduction in the condensation temperature of steam. At the same time, condensation temperature of solvent rises because of an increase in its mole fraction (y_{solv}) and, hence, its partial pressure (P_{solv}).

With further reduction in temperature, steam continues to condense and the vapor phase becomes increasingly richer in solvent. Therefore, the difference between the cell temperature and the solvent condensation temperature keeps reducing. When the cell temperature reduces to 393°F and vapor mole fraction of diluent (y_{solv}) increases to 0.4252, both components have partial pressures equal to their saturation pressures and condense together **(Fig. 4).** This is the condensation temperature of the steam/solvent mixture. At temperatures lower than this, steam and solvent (diluent) exist in liquid phase only.

The condensation temperature does not depend on the initial solvent concentration in the mixture. The mixture condenses when solvent mole fraction in the vapor phase increases to a critical value ($y_{solv} = y^*_{solv}$), where solvent partial pressure increases sufficiently and its condensation temperature becomes equal to the cell temperature (which is also equal to the steam's condensation temperature at its existing partial pressure). **Table 5** shows condensation temperature of the mixture for various solvents at 400 psi. The steam-solvent condensation temperature is always lower than the pure steam condensation temperature. It also shows the critical solvent mole fraction in the vapor phase at the condensation temperature (y^*_{solv}).

TABLE 5—CONDENSATION TEMPERATURE AND CRITICAL CONCENTRATIONS OF VARIOUS SOLVENTS

	Steam Only	Propane	Butane	Pentane	Hexane	Heptane	Diluent	Octane	Decane	Syncrude
Boundary temperature (°F)	444.59	161.73	280.11	336.05	371.70	395.76	393.65	411.61	429.35	443.68
Critical concentration (y^*)	—	0.9898	0.8768	0.7203	0.5572	0.4110	0.4252	0.2956	0.1467	0.0108

Pressure = 400 psi.

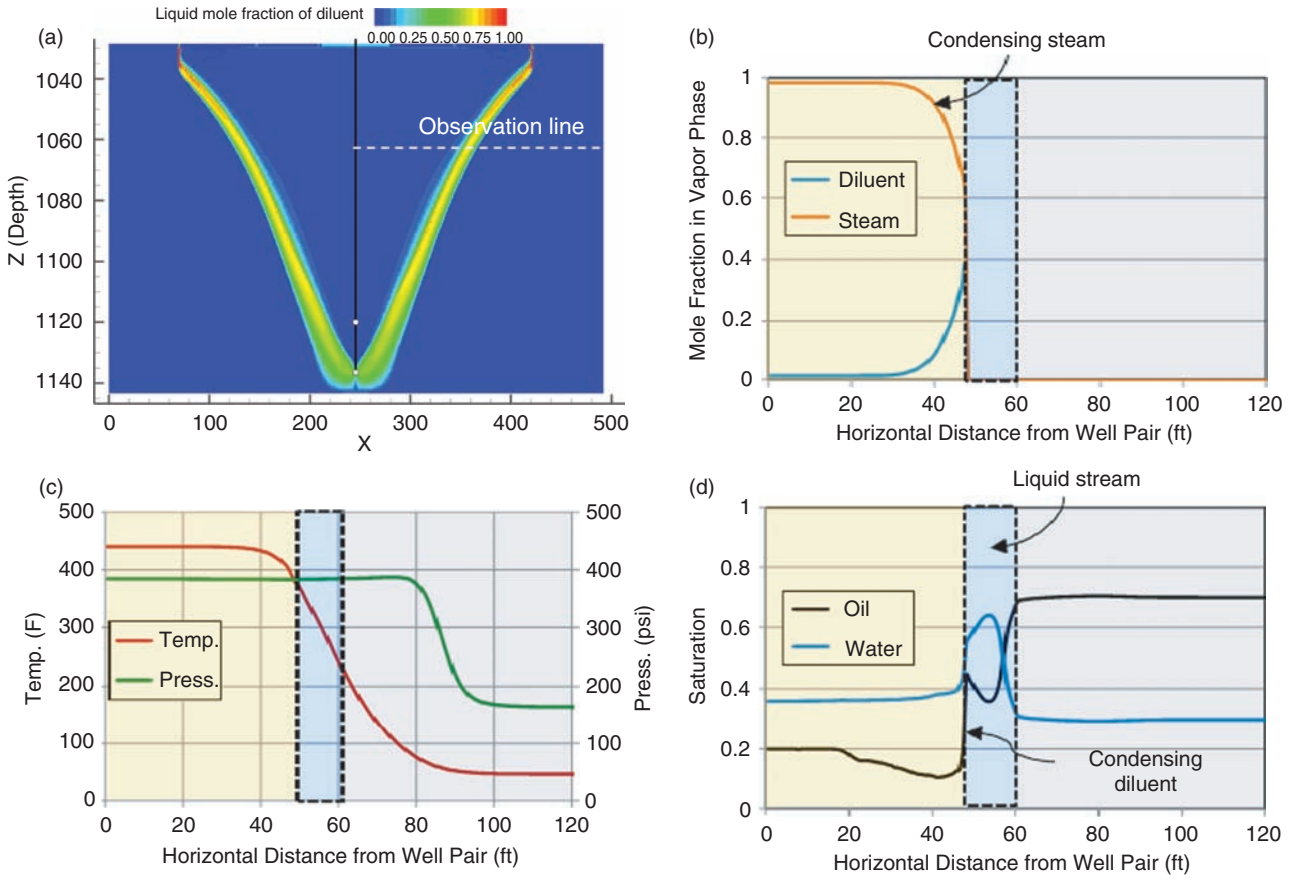

Fig. 5—Details of oil recovery with steam/diluent coinjection. (a) A cross section of the steam chamber. (b) Variation in temperature and pressure along the observation line. Temperature declines near the chamber boundary because of condensation of the steam/solvent mixture. (c) Variation in the composition of the vapor phase. Because of condensation of steam, the vapor phase becomes increasingly richer in solvent toward the chamber boundary. (d) Formation of a liquid stream outside the chamber boundary. The liquid stream includes a condensed solvent stream immediately adjacent to chamber boundary.

Hexane has often been recommended as the most suitable solvent (Nasr et al. 2003; McCormack 2009). Hexane's vapor pressure is similar to that of steam, so it is argued that steam and hexane would condense together and provide maximum benefits. However, because the solvent concentration in the injected mixture is typically much smaller than the critical solvent concentration, y^*_{solv}. Therefore, steam always starts condensing at a higher temperature compared with the solvent. Thus, the argument given in favor of hexane is invalid. Further, as it will be shown later, in the comparison of different solvents, that the lighter solvents are preferred.

Next, the oil-recovery mechanism for a steam/solvent-coinjection process is explained by use of diluent as the solvent. As in the case of SAGD, we investigate various parameters of interest along an observation line. In this case also, the steam chamber, the liquid stream, and the unperturbed region are demarcated in different colors.

Variation of Pressure and Temperature in the Reservoir (Fig. 5b). As in the case of pure-steam injection, the pressure and temperature in the central region of the steam chamber are invariant. Further, there is little change in the central region of steam chamber temperature because the solvent concentration is very small. Near the boundary of the chamber when temperature drops to the condensation temperature of steam, the steam starts condensing. Moving toward the chamber boundary, steam continues to condense and its partial pressure keeps dropping. The local temperature at any point corresponds to the prevailing partial pressure of steam and is lower than the saturated steam temperature at the injection pressure. The temperature at the boundary is the condensation temperature of the steam/solvent mixture. A drop in temperature (approximately 49°F) near the chamber boundary can be seen in Fig. 5b.

This drop in temperature near the chamber boundary region is a side effect of the solvent addition. Yuan et al. (2006) experimentally observed a drop in temperature and found that the presence of a small amount of the "volatile portion" altered the temperature profile in the dead-oil experiment and the steam chamber appeared smaller than would be expected.

As in SAGD, the region beyond the steam-chamber boundary is conductively heated. The temperature declines as we move away from the boundary.

Variation in Saturations. Fig. 5d shows the variation of the oil and water saturations along the observation line. Unlike steam-only injection, in this case the phase saturations and their composition vary in the steam chamber.

The steam/solvent mixture is essentially in the vapor phase in the central region of the chamber. Near the chamber boundary, steam starts condensing when the local temperature drops to the condensation temperature. A condensation zone forms from this point up to the chamber boundary. The condensation of steam causes the vapor phase to be richer in the solvent in the condensation zone. At the boundary of the chamber, the solvent concentration in the vapor phase reaches its critical value ($y_{solv} = y^*_{solv}$) and the mixture condenses, as noted previously.

Even though the solvent concentration in the injected fluid is small (approximately 0.86%), its concentration in the vapor phase becomes high near the chamber boundary (approximately 43% in Fig. 5c). This increase in solvent mole fraction in the vapor phase near the chamber boundary is often referred to as solvent vapor "accumulation" in the literature, which in our opinion is a misnomer. Increase in solvent mole fraction is only a consequence of steam condensation. There is no net influx of solvent in this region.

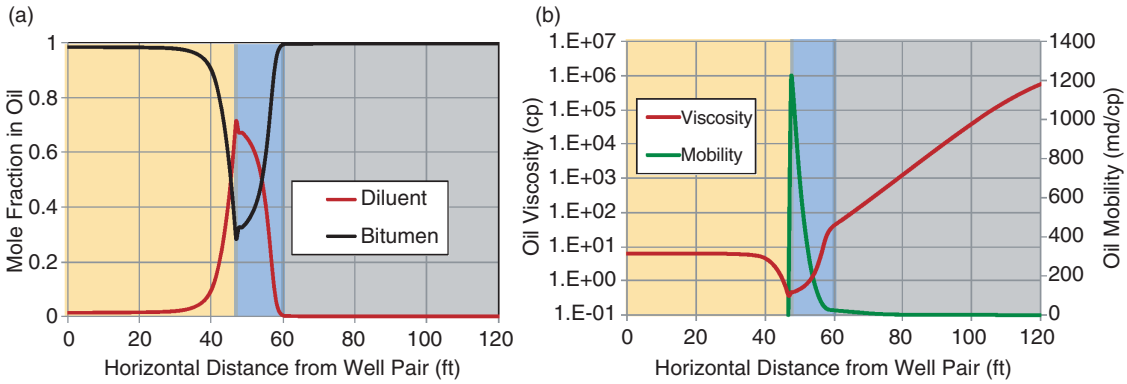

Fig. 6—(a) Variation in oil-phase composition along the observation line. Solvent mixes with the heated oil in the drainage region. (b) Variation in oil viscosity and mobility. Mixing of heated oil with the condensed solvent causes an additional reduction in the oil viscosity compared with steam only case (Fig. 3d).

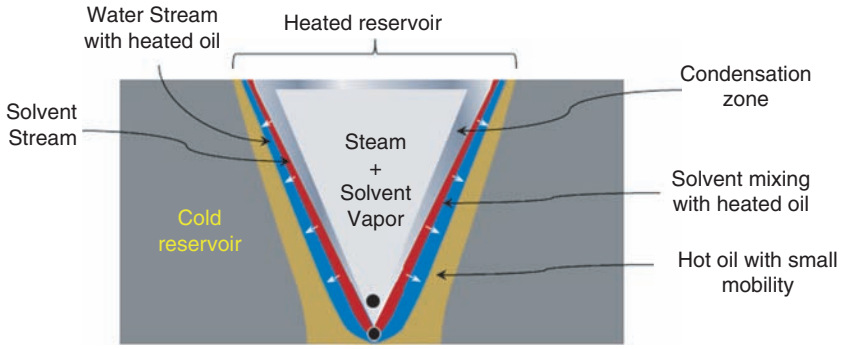

Fig. 7—A mechanistic model showing distinct regions of the reservoir during steam-solvent co-injection process and the important phenomena occurring there. The injected steam-solvent mixture condenses near the chamber boundary in the condensation zone. Condensation of solvent and steam leads to the formation of a liquid stream adjacent to the chamber boundary. The fluid mobility is limited to the liquid stream. Solvent and water form separate streams. The solvent stream lies above the water stream because of its lower density. Solvent mixes with heated oil and causes an incremental reduction in oil viscosity and hence leads to a faster production rate.

With increasing partial pressure of solvent in the condensation zone (and decline in temperature), its solubility in residual bitumen in the steam chamber increases. Thus, the solvent concentration in bitumen increases in the condensation zone and it reaches the peak concentration at the boundary of the steam chamber. This is reflected in increasing oil saturation in the condensation zone (Fig. 5d) and in increasing solvent concentration in oil in that zone **(Fig. 6a).**

Unlike the steam only case, where steam condenses at the location where the temperature is at the saturated condition, now have a condensation zone near the chamber boundary where steam and solvent condense. This leads to a small increase in liquid saturations in this zone. Movable (or mobile) liquid is present in this zone as well. However, liquid mobility in this zone is small because of the small liquid saturations. Practically, liquid mobility is still limited to the drainage region that lies adjacent to the steam chamber.

Condensed steam and solvent both drain outside of the steam chamber. These fluids are immiscible and have different densities. Therefore, they segregate and form separate streams. Because solvent density is lower than that of water (specific density of diluent is 0.77), the solvent stream lies above the water stream (along the tilted boundary of the chamber). Thus, in case of steam/solvent coinjection, the liquid stream contains an additional stream of condensed solvent (Fig. 5d).

Impact of Solvent on Viscosity. Because the condensed solvent is miscible with oil, the oil phase consists of two components: bitumen and condensed solvent. Fig. 6a shows the composition of oil. As in the case of steam-only injection, fluid mobility is limited to the liquid stream (Fig. 6b). In this region, the heated oil, condensed solvent, and water flow to the producer. The condensed solvent mixes with the heated oil.

The solvent viscosity is low (Table 3). Mixing of solvent with bitumen further reduces the heated-oil viscosity. This is evident from a change in the slope of the viscosity curve (Fig. 6b) in the drainage region. This additional reduction in viscosity more than offsets the effect of reduced temperature at the chamber boundary. The bitumen viscosity at the midpoint of the drainage region for steam-only injection is 22.5 cp (Fig. 3d). Even after a 49°F drop in temperature at the chamber boundary (compared with the steam-only case), the bitumen viscosity at the midpoint of the drainage region decreases to approximately 1 cp because of mixing with the solvent (Fig. 6b). This additional reduction in the oil viscosity results in a higher oil production rate.

Fig. 7 summarizes the steam/solvent-coinjection process described earlier in the form of a simple picture, or mechanistic model. It shows the different regions of the reservoir and the important phenomena occurring there.

Impact of Solvent on ROS. With continued steam/solvent coinjection, the chamber expands and the whole arrangement shifts laterally outward. **Fig. 8** shows oil saturation along the observation line at two different times. The peak in oil saturation near the steam-chamber boundary is a result of solvent condensation there. With continued steam/solvent coinjection, the steam chamber expands and the previous liquid stream becomes a part of the steam chamber. The temperature in that region rises and, therefore, part of the condensed solvent evaporates. This leads to a lowering of ROS in the steam chamber and thus causes improved oil recovery.

Fig. 9a plots ROS in the steam chamber along the observation line. It also plots the peak solvent concentration that occurred at that location. Fig. 9b plots ROS vs. historic peak solvent

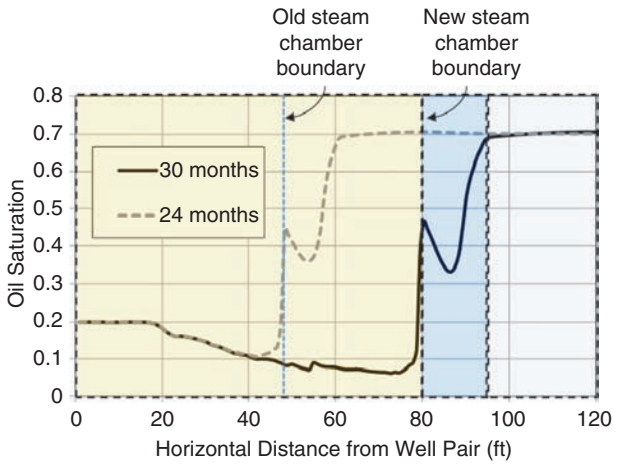

Fig. 8—Illustration of reduction in ROS. With continued steam/solvent injection, the chamber expands. The condensed solvent evaporates because of increase in temperature. Therefore, the ROS in the steam chamber reduces.

concentration for several locations inside the steam chamber. A strong relationship between the two is evident in both figures. Lowering of ROS is caused by evaporation of the condensed solvent from the oil. The higher the peak solvent concentration at a location in solvent stream, the lower the ROS at that location. Slight scatter in data in Fig. 9b may be attributed to difficulty in ascertaining the peak solvent concentration at a location.

The mechanism of an improvement in ultimate oil recovery was not understood previously (Nasr and Ayodele 2006). There are several instances in the literature (Gates 2007; Ardali et al. 2011) that model the steam/solvent-coinjection process by use of small ROS to gas (S_{org} of approximately 0.005) or solvent-concentration-dependent residual saturation (Ivory et al. 2010). An inappropriate representation of ROS in numerical simulations may result in erroneous conclusions. We show that a small S_{org} is not needed to reproduce experimental observations of lower S_{org} with solvent, and greater ultimate recovery. By use of the same value of S_{org} as in the steam-only injection, we obtain smaller ROS in the steam chamber because of vaporization of the condensed solvent.

Our explanation of improvement in ultimate recovery is corroborated by experiments conducted by Nasr and Ayodele (2006). They report experimentally measured ROSs for SAGD and steam/solvent coinjection (for two different concentrations). They observed a lower ROS in the steam chamber for a steam/solvent-coinjection process. Their other experiment shows the composition of ROS in the steam chamber. A low solvent concentration in the residual oil in the steam chamber was observed. These experimental observations support our conclusion that evaporation of the condensed solvent causes a reduction in the ROS, which leads to an improvement in the ultimate recovery.

Thus, in summary, adding solvent results in greater oil rate because of additional reduction in oil viscosity and lowering of ROS in the steam chamber. The latter effect also leads to improved ultimate recovery.

Comparison of Performances of Different Solvents

Fig. 10 compares performance of all solvents investigated in this study. Butane provides the highest oil rate and the highest recovery. Except for propane, the performance (in terms of oil rate and cumulative production at a given time) of the solvent improves consistently as the solvent becomes lighter.

As seen from Fig. 2 and Table 5, propane is volatile and condenses at a low temperature. It does not condense completely in the steam chamber and acts partially as a noncondensable gas. Therefore, it is not a solvent similar to the other solvents considered in this study. Several researchers have investigated the impact of injecting noncondensable gas with steam (Yuan et al. 2006; Sharma et al. 2012). They demonstrate that a noncondensable gas slows down the growth of the steam chamber. Therefore, propane lowers steam-injection rate and provides low oil rates. Still, for a given amount of cumulative steam injection, it provides the best cumulative oil production.

To analyze results of other solvents, **Fig. 11a** compares viscosity profiles for three common solvents. As is evident, all the solvents cause additional reduction in viscosity compared with steam-only injection. Viscosity reduction by mixing with solvent more than compensates for the reduced temperature near the chamber boundary.

A lighter solvent has a lower viscosity (Table 3). In addition, a lighter solvent also has a higher molar concentration of solvent in the mixing zone because of higher moles of solvent injected (corresponding to the same weight percent of solvent as shown in Table 4). Thus, a lighter solvent causes a greater reduction in the viscosity of the heated-oil viscosity. Even after accounting for the greater temperature reduction, a lighter solvent is preferable for viscosity reduction (Fig. 11a).

Fig. 11b compares ROS profiles for three common solvents. Clearly, lighter solvents lead to a lower ROS. As indicated in the preceding paragraph, a lighter solvent has a higher molar concentration of solvent in oil in the mixing zone. Moreover, it also possesses a higher volatility. Because of these factors, a lighter solvent leads to a lower ROS and hence to a greater ultimate recovery.

Therefore, accounting for both the mechanisms, the lightest condensable solvent (butane, under the conditions investigated) causes the greatest reduction in oil viscosity and also results in the lowest ROS. Thus, it provides the most favorable results in terms of enhancements in oil rate and oil recovery. This is contrary to prior claims in the literature noted earlier, where Hexane has been recommended as the most suitable solvent.

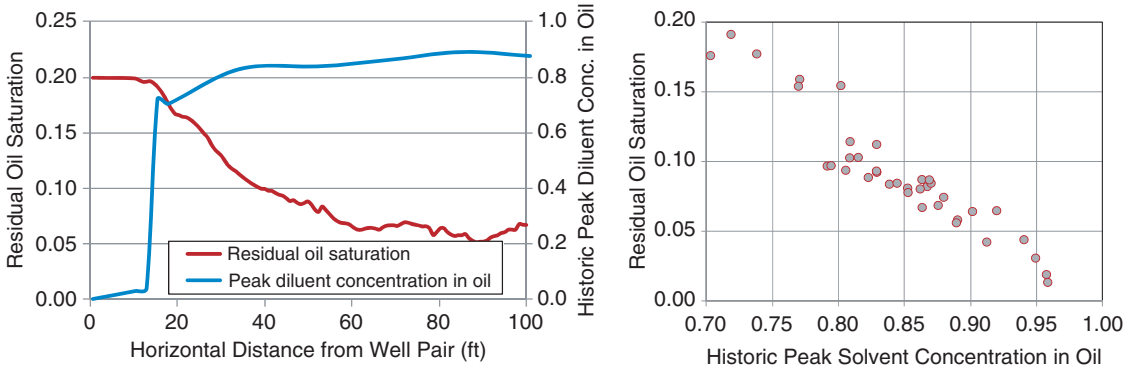

Fig. 9—(a) ROS at a location depends on the historic peak solvent concentration at that location. The higher the peak solvent concentration in the oil, the lower is the ROS. (b) ROS vs. peak solvent concentration. Slight scatter in data may be attributed to difficulty in ascertaining the peak solvent concentration at a location.

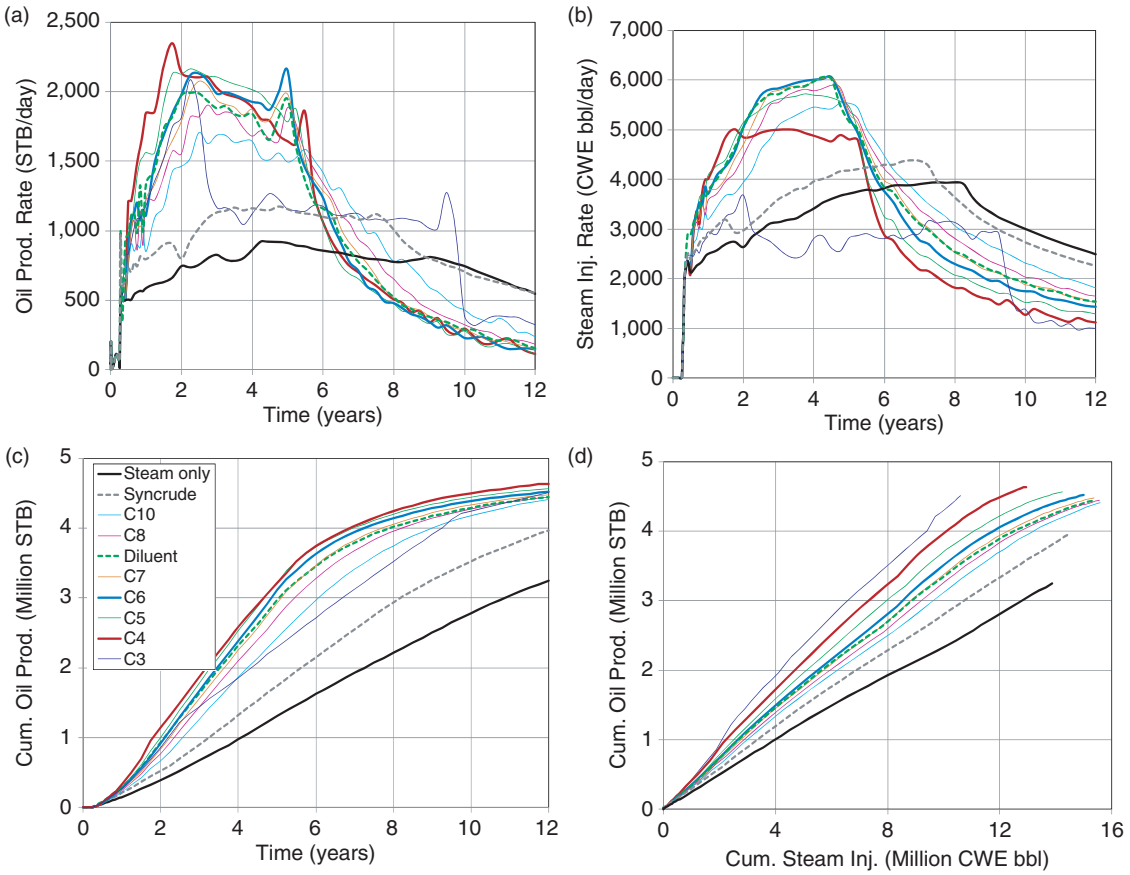

Fig. 10—A comparison of the performance of different solvents. (a) Oil-production rate vs. time. (b) Steam-injection rate vs. time. (c) Cumulative oil production vs. time. (d) Cumulative oil production vs. cumulative steam injection. Except for propane, which is partially noncondensable, performance of solvent in terms of oil rate and cumulative production improves as the solvent becomes lighter.

Limitations of the Current Study and Future Work

The current study does not include transverse dispersion explicitly and relies on numerical dispersion for mixing of the condensed solvent with heated oil. However, solvent dispersion has a small effect on the steam/solvent-coinjection process because it is dominated by thermal diffusion (Deng et al. 2010). The quantification of mixing occurring in the field operations is still uncertain, and it is a challenge to scale up laboratory-scale mixing to the field scale (Boone et al. 2011).

The results in this study are for a fixed operating condition: a single constant injection pressure. Investigating the process for a broader range of operating conditions would be invaluable in generalizing the results. Also, the effect of solution gas was not included in this study for simplicity and ease of comparison with independent phase-behavior calculations. The effect of solution gas should be included in the future. In addition, as noted earlier, a single pseudocomponent was used to represent the industrial solvents, diluent and syncrude. Use of a multicomponent solvent model would be more representative for field design.

Summary and Conclusions

We present details of the steam/solvent-coinjection-process mechanism. A mechanistic model is developed in this study that describes the most important phenomena occurring in the different regions of the reservoir and their implications for oil recovery.

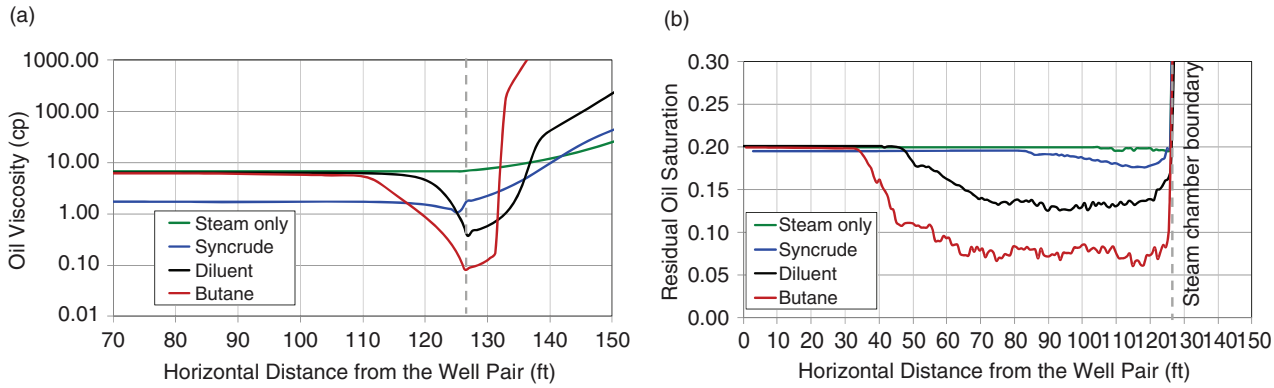

Fig. 11—Evaluating the impacts of common solvents. (a) A lighter solvent causes a greater reduction in the oil viscosity. (b) A lighter solvent also results in a smaller ROS in the steam chamber. Therefore, a lighter solvent leads to a greater oil-production rate and a greater ultimate recovery.

We compare performances of various solvents and explain the reasons for the observed differences. The model identifies the solvent properties and operating conditions that improve oil rate and maximize incremental oil production. An improved understanding of the process mechanism will facilitate optimal operating-parameters selection, enhancing commercial applicability of the process.

The key findings of this study are:

- For the typical concentration of solvent in the injected mixture, steam starts condensing at a higher temperature. Steam continues to condense toward the chamber boundary, and consequently the vapor phase becomes increasingly richer in solvent. At the boundary, the temperature becomes equal to the condensation temperature of both steam and solvent and both condense simultaneously. This condensation of the steam/solvent mixture is accompanied by a reduction in temperature near the condensation region. However, the steam chamber temperature (in its central region) remains nearly unchanged.
- The condensed steam/solvent mixture drains outside the chamber boundary, leading to the formation of a mobile liquid stream where heated oil, condensed solvent, and water flow together to the production well.
- The condensed solvent mixes with the heated oil and reduces its viscosity further. The additional reduction in viscosity by solvent more than offsets the impact of reduced temperature near the chamber boundary and results in a higher oil-production rate compared with steam-only injection.
- When the steam chamber expands laterally because of continued injection and temperature in what was previously the drainage region increases, part of the condensed solvent mixed with oil evaporates. This lowers the ROS in the steam chamber. The higher the solvent concentration in oil at a location, the greater the reduction in the ROS at that location, leading to improved ultimate recovery.
- All solvents investigated in this study provide sufficient additional reduction in oil viscosity to offset the detrimental effect of reduced temperature near the steam chamber boundary. Hence, they all yield faster drainage rate compared with steam-only injection.
- A lighter solvent has a lower viscosity, a higher volatility and a higher molar concentration of solvent in the drainage region. Thus, a lighter solvent causes a greater reduction in the viscosity of the heated oil and also leads to a lower residual oil saturation. Therefore, the lightest condensable solvent (butane, under the conditions investigated) provides the most favorable results in terms of enhancements in oil rate and oil recovery.

Thus, it provides the highest oil rate and oil recovery. This paper, for the first time, provides the details of the steam/solvent-coinjection-process mechanism and explains the increase in ultimate recovery during the process. It demonstrates that it is unnecessary to use small values of ROS in simulation studies. It also demonstrates that the lightest condensable solvent is the most suitable solvent, which is different from prior claims in the literature.

Nomenclature

A_i = first Antoine coefficient of the component i
B_i = second Antoine coefficient of the component i
C_i = third Antoine coefficient of the component i
k = permeability, md
k_r^o = relative permeability to oil
K_i = phase equilibrium constant for component i
P_i = vapor pressure of component i, mm Hg
P_{solv} = partial pressure of solvent, psi
P_{stm} = partial pressure of steam, psi
P_t = total pressure, psi
S_{org} = residual oil saturation to gas
T = temperature, K
x_i = mole fraction of component i in oil phase
y_{solv} = mole fraction of solvent in vapor phase
y_{solv}^* = critical mole fraction of solvent in vapor phase
y_{stm} = mole fraction of steam in vapor phase
μ_o = viscosity of oil, cp
μ_{oi} = viscosity of component i in oil phase, cp

References

Aherne, A. L. and Maini, B. 2008. Fluid Movement in the SAGD Process: A Review of the Dover Project. *J. Cdn. Pet. Tech.* **47** (1): 31–37. http://dx.doi.org/10.2118/08-01-31.

Ardali, M., Barrufet, M. A. and Mamora, D. D. 2012. A Critical Review of Hybrid Steam/Solvent Processes to Recover Heavy Oil. Paper SPE 159257 presented at SPE Annual Technical Conference and Exhibition, San Antonio, Texas, 8–10 October. http://dx.doi.org/10.2118/159257-MS.

Ardali, M., Mamora, M. and Barrufet, M. 2011. Experimental Study of Co-injection of Potential Solvents with Steam to Enhance SAGD Process. Paper SPE 144598 presented at SPE Western North American Regional Meeting, Anchorage, Alaska, 7–11 May. http://dx.doi.org/10.2118/144598-MS.

Birrell, G. E. 2001. Heat Transfer Ahead of SAGD Steam Chamber, a Study of Thermocouple Data From Phase B of the Underground Test Facility (Dover Project). Paper SPE 71503 presented at SPE Annual Technical Conference and Exhibition, New Orleans, Louisiana, 30 September–3 October. http://dx.doi.org/10.2118/71503-MS.

Boak, J. and Palmgren, C. 2004. Preliminary Numerical Analysis for a Naptha Co-Injection Test During SAGD. Paper SPE 2004-001 presented at Canadian International Petroleum Conference, Calgary, Alberta, Canada, 1–8 June. http://dx.doi.org/10.2118/2004-001.

Boone, T. J., Wattenbarger, C., Clingman, S., et al. 2011. An Integrated Technology Development Plan for Solvent-based Recovery of Heavy Oil. Paper SPE 150706 presented at SPE Heavy Oil Conference and Exhibition, Kuwait City, Kuwait, 12–14 December. http://dx.doi.org/10.2118/150706-MS.

Bracho, L. G. and Oquendo, O. A. 1991. Steam-Solvent Injection, Well LSJ-4057, Tia Juana Field, Western Venezuela. Paper SPE 21530 presented at the SPE International Thermal Operations Symposium, Bakersfield, California, 7–8 February. http://dx.doi.org/10.2118/21530-MS.

Butler, R. M. 1994. Steam-assisted Gravity Drainage: Concept, Development, Performance and Future. *J. Cdn. Pet. Tech.* **33** (2): 44–50. http://dx.doi.org/10.2118/94-02-05.

Chien, M. C. H., Lee, S. T. and Chen, W. H. 1985. A New Fully Implicit Compositional Simulator. Paper SPE 13385 presented at the SPE Reservoir Simulation Symposium, Dallas, Texas, 10–13 February. http://dx.doi.org/10.2118/13385-MS.

Deng, X., Huang, H., Zhao, L., et al. 2010. Simulating the ES-SAGD Process with Solvent Mixture in Athabasca Reservoirs. *J. Cdn. Pet. Tech.* **49** (1): 38–46. http://dx.doi.org/10.2118/132488-PA.

Dong, L. 2012. Effect of Vapor-Liquid Phase Behavior of Steam-Light Hydrocarbon Systems on Steam Assisted Gravity Drainage Process for Bitumen Recovery. *Fuel* **95** (May): 159–168. http://dx.doi.org/10.1016/j.fuel.2011.10.044.

Edmunds, N., Moini, B. and Peterson, J. 2009. Advanced Solvent-Additive Processes via Genetic Optimization. Paper SPE 2009-115 presented at Canadian International Petroleum Conference, Calgary, Alberta, Canada, 16–8 June. http://dx.doi.org/10.2118/2009-115.

Gates, I. D. 2007. Oil Phase Viscosity Behavior in Expanding-Solvent Steam-Assisted Gravity Drainage. *J. Pet. Sci. Eng.* **59** (1–2): 123–134. http://dx.doi.org/10.1016/j.petrol.2007.03.006.

Gupta, S., Gittins, S. and Picherack, P. 2005. Field Implementation of Solvent Aided Process. *J Cdn. Pet. Tech.* **44** (11): 8–13. http://dx.doi.org/10.2118/05-11-TN1.

Gupta, S. C. and Gittins, S. D. 2006. Christina Lake Solvent Aided Process Pilot. *J Cdn. Pet. Tech.* **45** (9): 15–18. http://dx.doi.org/10.2118/06-09-TN.

Hong, K. C. and Hsueh, L. 1987. Comparison of K-Value Calculation Methods in Compositional Steamflood Simulation. *SPE Res Eval & Eng* **2** (2): 249–257. http://dx.doi.org/10.2118/12750-PA.

Ito, Y. and Suzuki, S. 1999. Numerical Simulation of the SAGD Process in the Hangingstone Oil Sands Reservoir. *J. Cdn. Pet. Tech.* **38** (9): 57,2–57,14. http://dx.doi.org/10.2118/99-09-02.

Ivory, J., Frauenfeld T. and Jossy, C. 2010. Thermal Solvent Reflux and Thermal Solvent Hybrid Experiments. *J. Cdn. Pet. Tech.* **49** (2): 23–31. http://dx.doi.org/10.2118/133202-PA.

Jimenez, J. 2008. The Field Performance of SAGD Projects in Canada. Paper SPE 12860 presented at International Petroleum Technology Conference, Kuala Lumpur, Malaysia, 3–5 December. http://dx.doi.org/10.2523/12860-MS.

Leaute, R. P. and Carey, B. S. 2007. Liquid Addition to Steam for Enhancing Recovery (LASER) of Bitumen with CSS: Results from the First Pilot Cycle. *J. Cdn. Pet. Tech.* **46** (9): 22–30. http://dx.doi.org/10.2118/07-09-01.

McCormack, M. E. 2009. Design of Steam-Hexane Injection Wells For Gravity Drainage Systems. *J. Cdn. Pet. Tech.* **48** (1): 22–28. http://dx.doi.org/10.2118/09-01-22.

Nasr, T. N., Beaulieu, G., Golbeck, H., et al. 2003. Novel Expanding Solvent-SAGD Process "ES-SAGD." *J. Cdn. Pet. Tech.* **42** (1): 13–16. http://dx.doi.org/10.2118/03-01-TN.

Nasr, T. N. and Ayodele, O. R. 2005. Thermal Techniques for the Recovery of Heavy Oil and Bitumen. Paper SPE 97488 presented at SPE International Improved Oil Recovery Conference in Asia Pacific, Kuala Lumpur, Malaysia, 5–6 December. http://dx.doi.org/10.2118/97488-MS.

Nasr, T. N. and Ayodele, O. R. 2006. New Hybrid Steam-Solvent Processes for the Recovery of Heavy Oil and Bitumen. Paper SPE 101717 presented at Abu Dhabi International Petroleum Exhibition and Conference, Abu Dhabi, UAE, 5–8 November. http://dx.doi.org/10.2118/101717-MS.

NIST. 2011. NIST Chemistry WebBook, http://webbook.nist.gov/chemistry (accessed March 2013).

Orr, B. 2009. ES-SAGD; Past, Present and Future. Paper SPE 129518-STU presented at SPE Annual Technical Conference and Exhibition, New Orleans, Louisiana, 4–7 October.

Reid, R. C., Prausnitz, J. M. and Poling B. E. 1986. *The Properties of Gases and Liquids*, fourth edition. New York City, New York: McGraw-Hill.

Sharma, J., Moore, R.G. and Mehta, R. 2012. Effect of Methane Co-injection in SAGD–Analytical and Simulation Study. *SPE J.* **17** (3): 687–704. http://dx.doi.org/10.2118/148917-PA.

Sharma, J. and Gates, I. D. 2011. Convection at the Edge of a Steam-Assisted-Gravity-Drainage Steam Chamber. *SPE J.* **16** (3): 503–512. http://dx.doi.org/10.2118/142432-PA.

Yuan, J. Y., Law, D. H. S. and Nasr, T. N. 2006. Impacts of Gas on SAGD: History Matching of Lab Scale Tests. *J. Cdn. Pet. Tech.* **45** (1): 503–512. http://dx.doi.org/10.2118/06-01-01.

Raman K. Jha is a research engineer for Chevron Energy Technology Company in Houston. He holds MS and PhD degrees from the University of Texas at Austin and a BTech degree from Indian School of Mines, Dhanbad, all in petroleum engineering. Jha's research interests include heavy-oil-recovery techniques, enhanced oil recovery, reservoir simulation, and hydrocarbon phase behavior.

Mridul Kumar is a Principal Advisor and Fellow with Chevron Energy Technology Company. He is currently the Unit Manager for Reservoir Performance Products, responsible for research, development, deployment, and support of Chevron's reservoir engineering tools, workflows, and technologies. Kumar is also a member of Chevron's reserves advisory committee. He has contributed to the success of Chevron's key heavy oil projects. Kumar holds a BTech degree (with distinction) from the Indian Institute of Technology in Kanpur, and MS and PhD degrees from the Pennsylvania State University, all in mechanical engineering. He has co-authored 50 papers and four patents, and has presented invited seminars worldwide. Kumar is a SPE Distinguished Member, and has been a SPE Distinguished Lecturer. He cochaired the 2009 SPE Forum on Heavy Oil and coauthored the SPE Reprint volume 61 on Heavy Oil Recovery (2008). Kumar received the 2002 SPE Western Region Technical Achievement Award, and was President of the SPE Golden Gate Section in 2001 through 2002.

Ian Benson is a reservoir engineer for Chevron Energy Technology Company in Houston. His research interests include heavy-oil-recovery techniques, reservoir simulation, field studies, and high-temperature horizontal-well designs and equipment. Benson holds an MS degree from the University of Texas at Austin and a BS degree from the University of Alberta, Edmonton, Alberta, Canada, both in petroleum engineering.

Ed Hanzlik is a senior consultant, heavy oil, with Chevron Energy Technology Company. He has more than 40 years of industry experience and has been involved with projects in many heavy-oil-producing regions. Hanzlik has been actively involved with numerous SPE committees, including chairing the Annual Technical Conference and Exhibition Program Committee and the Distinguished Lecturer Committee.